

Supporting information for

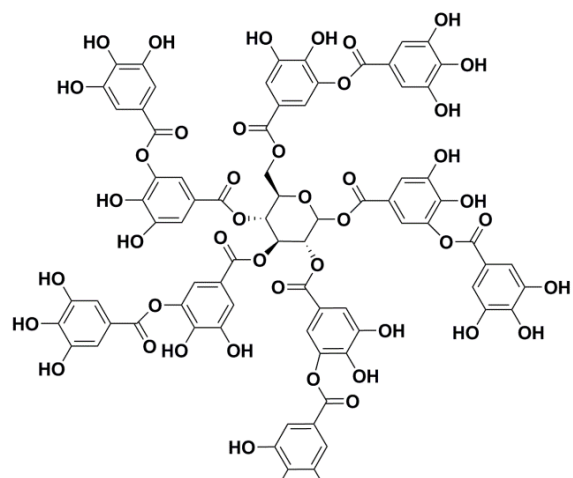
Microwave-assisted hydrothermal synthesis of UV-emitting carbon dots from tannic acid

Julin Joseph,^a Aji A. Anappara^{a*}

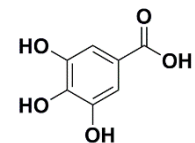
Department of Physics, NIT Calicut, Kerala, India.

Reference	$K_{SV} (M^{-1})$	Detection limit	Selectivity
<i>J. Mater. Chem.</i> , 2009, 19 , 7347-7353		4.8 ppb	High
<i>Adv. Funct. Mater.</i> , 2009, 19 , 905-917.	1.09×10^5	0.2 ppm	High
<i>Macromol. Rapid Commun.</i> , 2010, 31 , 834-839.	9.09×10^3	1 ppm	High
<i>Chem. Commun.</i> , 2011, 47 , 10046-10048.	2100		Low
<i>J. Photochem. Photobiol. A.</i> , 2011, 217 , 356-362.	5×10^4	2.3 ppb	Low
<i>ACS Appl. Mater. Interfaces.</i> , 2011, 3 , 1245-1253.	5.7×10^3	70 ppb	High
<i>Inorg. Chem.</i> , 2011, 50 , 1506-1512.	1×10^5		Low
<i>Chem. Commun.</i> , 2012, 48 , 7167-7169.	2.5×10^5	0.4 ppm	Low
<i>J. Mater. Chem.</i> , 2012, 22 , 11574-11582.	3.04×10^4	23 ppb	Moderate
<i>Chem. Commun.</i> , 2012, 48 , 5007-5009.	9.9×10^4	3-300 ppb	Low
<i>Angew. Chem. Int. Ed.</i> , 2013, 52 , 2881 -2885.	3.5×10^4	0.916 ppm	High
<i>ACS Appl. Mater. Interfaces.</i> , 2013, 5 , 672-679.	1.55×10^4	80.2 ppb	Moderate
<i>Chem. Commun.</i> , 2013, 49 , 4764-4766.	1.9×10^4		High
<i>J. Am. Chem. Soc.</i> , 2013, 135 , 17310-17313.	7.8×10^4	1 ppm	High
<i>J. Org. Chem.</i> , 2013, 78 , 1306-1310.	3.8×10^4		High
<i>Chem. Commun.</i> , 2014, 50 , 6031-6034.	5.28×10^4		Moderate
<i>ACS Appl. Mater. Interfaces.</i> , 2014, 6 , 10722-10728.	1.32×10^5	125 ppb	High
<i>Nanoscale.</i> , 2015, 7 , 1872-1878	2.850×10^4	0.068 ppm	Moderat
<i>Anal Methods.</i> , 2013, 5 , 6228-6233.	3.3×10^{-1}	0.229 ppm	High
<i>RSC Adv.</i> , 2014, 4 , 42066-42070.	3.3×10^{-1}	0.50 ppm	High
<i>J. Phys. Chem C.</i> , 2015, 119 , 13138-13143.		0.00229 ppm	Moderate
<i>RSC. Adv.</i> , 2014, 4 , 31994-31999.		75.6 ppb	Moderate
<i>J. Mater. Chem. A.</i> , 2016, 4 , 4161-4171.	3.18×10^4	0.05 ppm	High
<i>J. Photochem.. Photobiol B.</i> , 2016, 162 , 1-13.	9.68×10^6	0.19ppm	High

TableS1. List of different kinds of fluorophores used for picric acid detection.

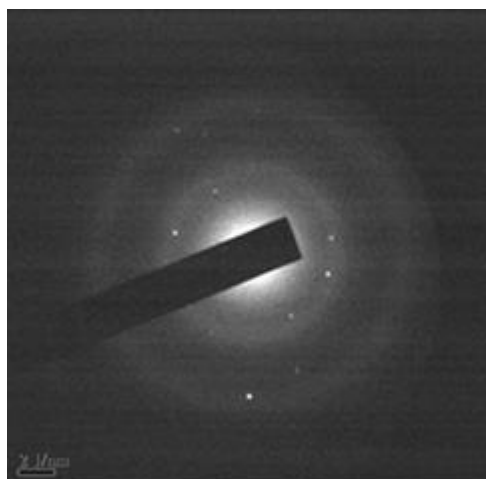


(a)

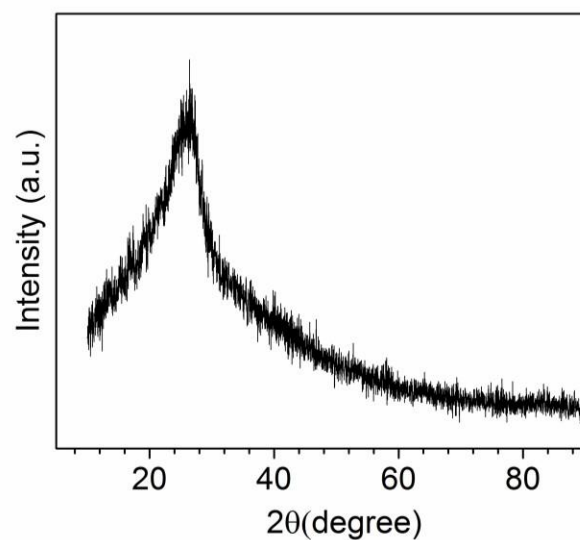


(b)

Fig.S1-(a) Representative chemical structure of tannic acid and (b) gallic acid.



(a)



(b)

Fig. S2-(a) Selected Area Electron Diffraction (SAED) of CDs obtained using Transmission Electron Microscopy (TEM). (b) XRD pattern of carbon dots.

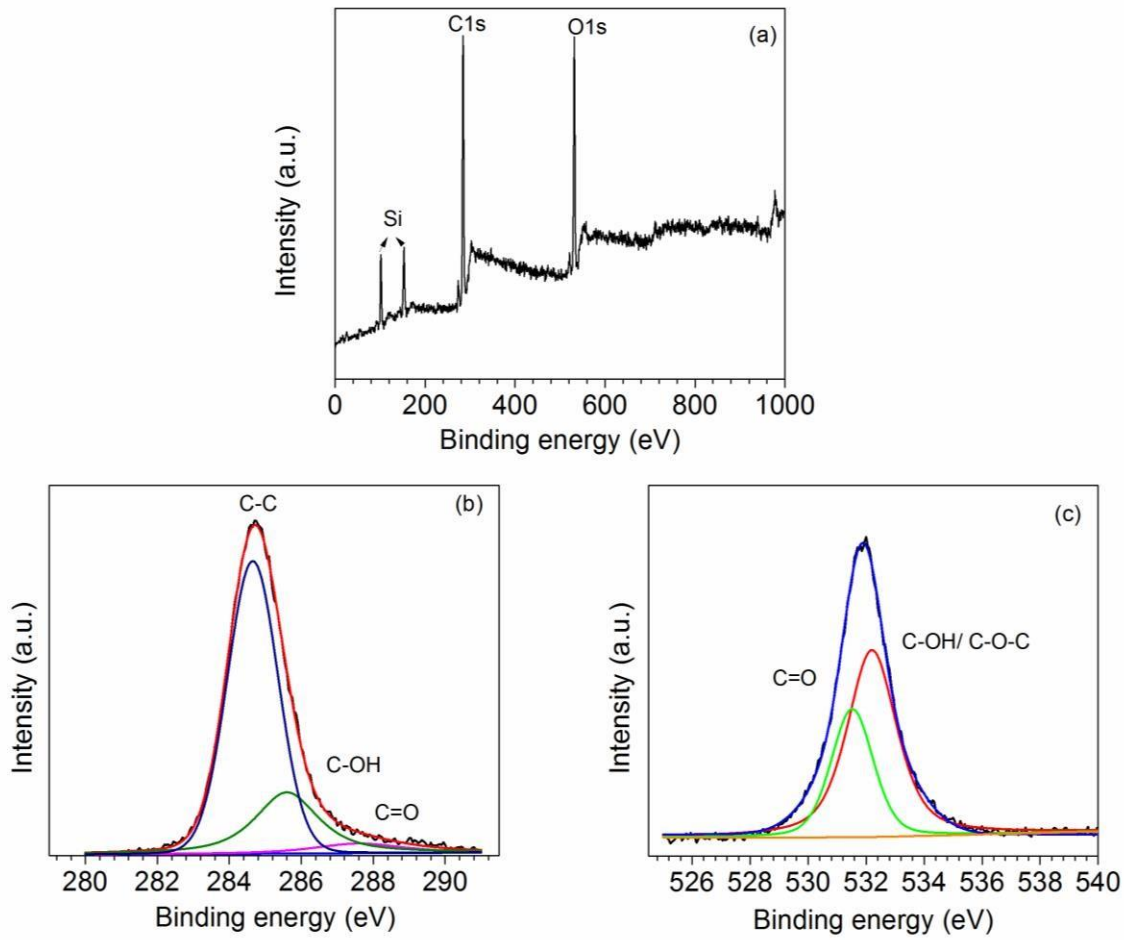


Fig.S3-(a) XPS scan spectra of the carbon dot dispersion spin-coated on to a glass plate followed by drying in air. The peaks at 103.6 eV and 150.8 eV are due to Si 2s and Si 2p resulted from glass plate. (b) C1s high resolution XPS spectra and (c) O1s high resolution spectra of CDs.

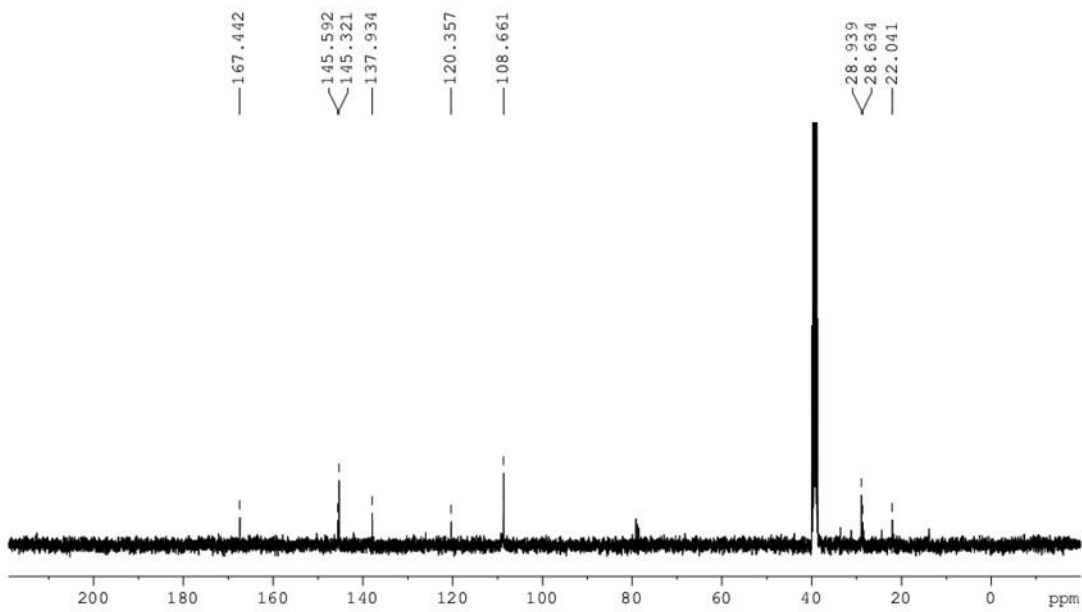


Fig.S4- ^{13}C NMR spectra of carbon nanodots. The spectra was collected after dissolving the nanoparticle powder in DMSO.

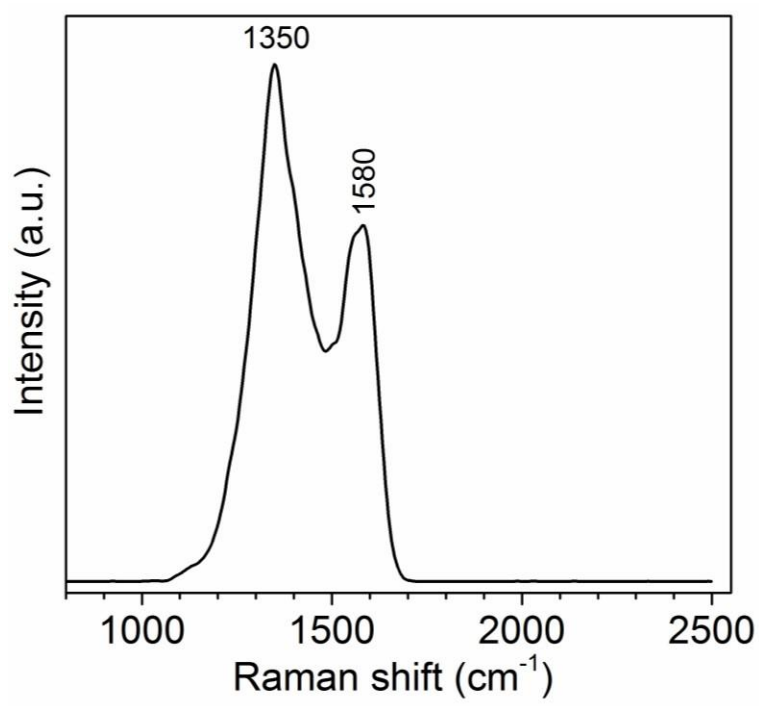


Fig.S5-Raman spectra of CDs. The excitation wavelength of the laser was chosen to be 532 nm. The peak at 1350 cm^{-1} represents D band and 1580 cm^{-1} corresponds to G band.

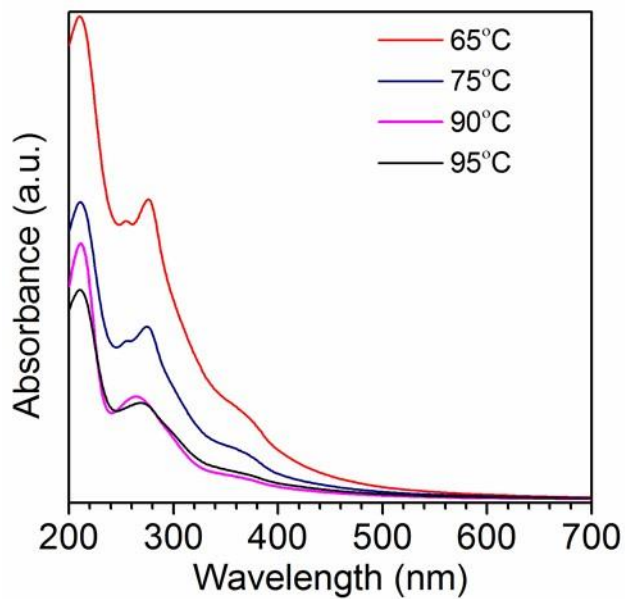


Fig.S6-UV-Vis absorption spectra of aqueous dispersion of carbon dots prepared by the microwave assisted hydrothermal route, performed at different temperatures.

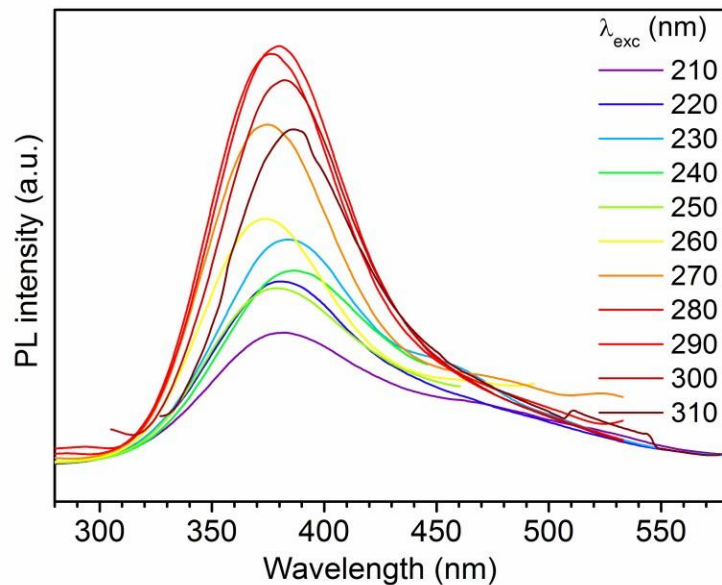


Fig.S7- Photoluminescence spectra of CDs after dispersing in water. The excitation wavelength was varied from 210 nm to 310 nm, in steps of 10 nm.

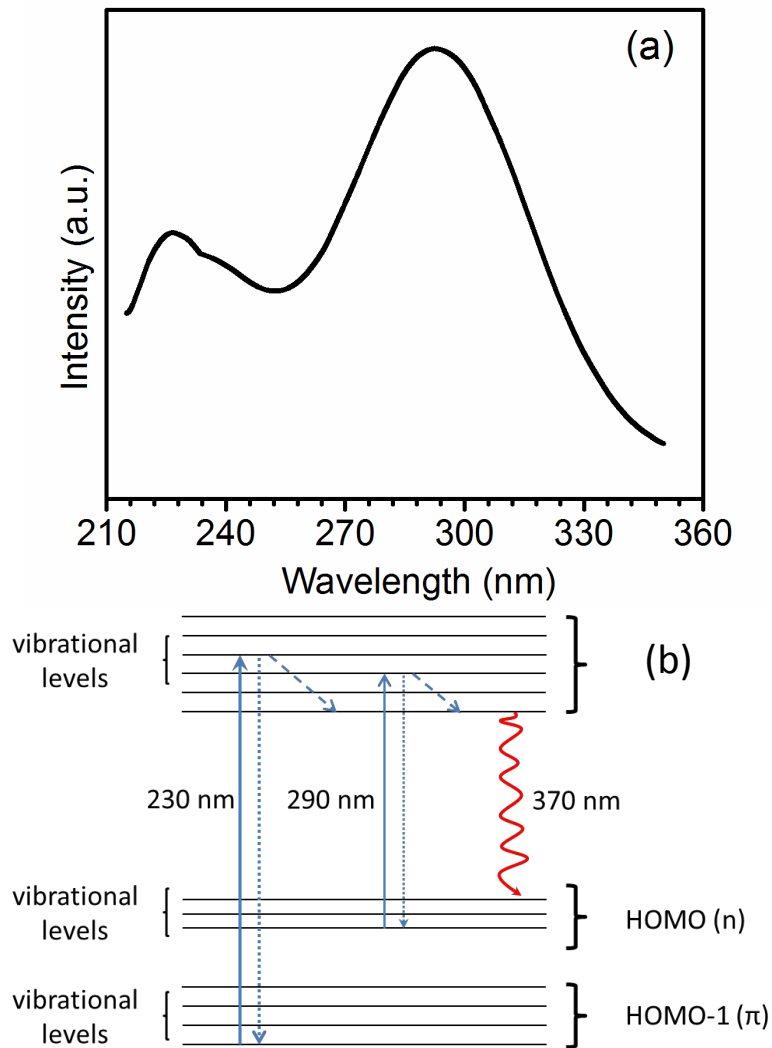


Fig S 8-a) The fluorescence excitation spectra of the CDs collected at the emission wavelength of 370 nm. (b)The schematic diagram representing the energy levels and the electronic transitions in the CDs.

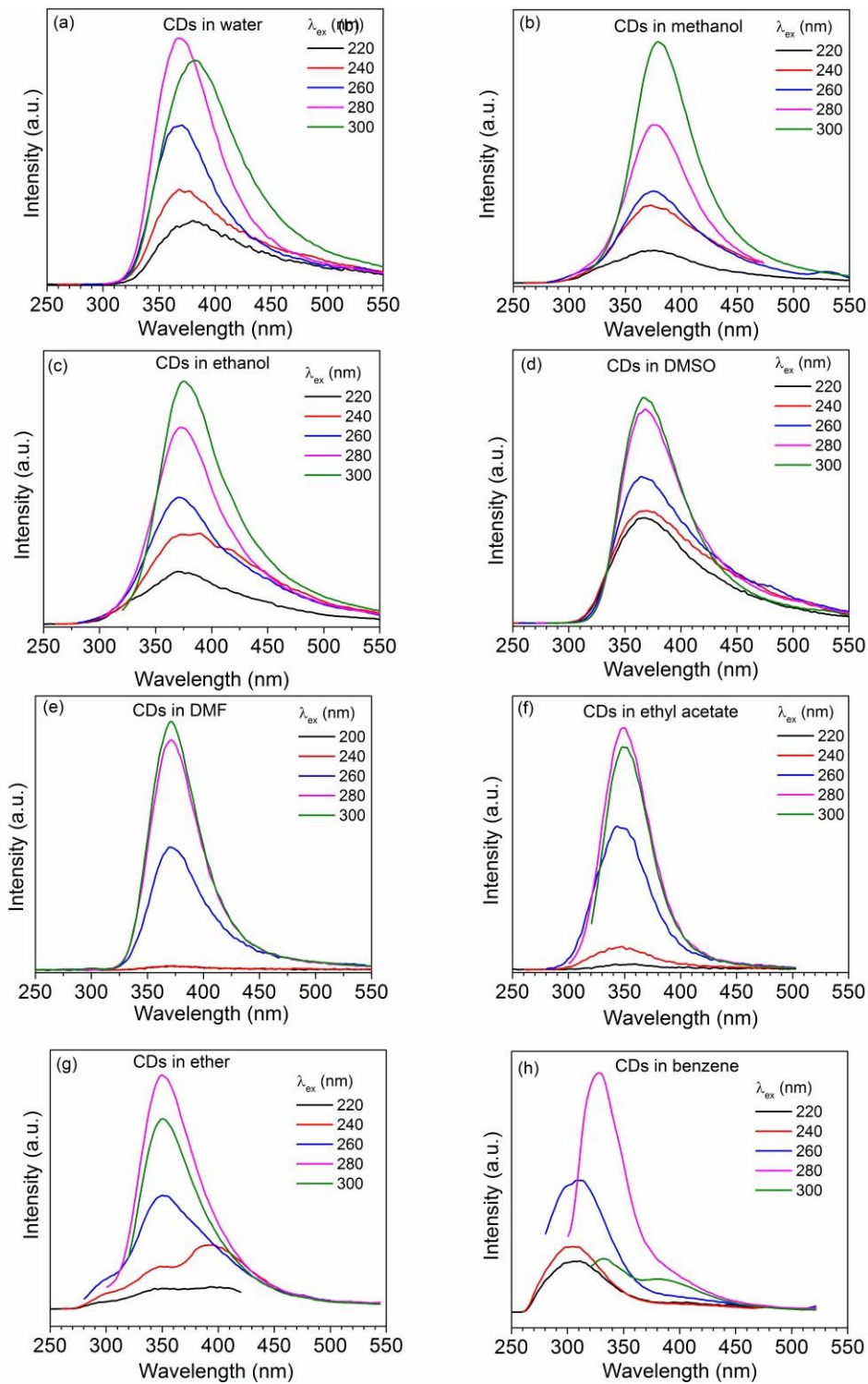


Fig.S9- Photoluminescence spectra of carbodots in different organic solvents. The concentration of the carbon nanoparticle taken is $6\mu\text{g/mL}$.

Solvent	$\lambda_{\text{ex}} (\text{nm})$	Quantum yield (%)	Relative polarity
Water	280	7.6	1
Methanol	298	6.8	0.762
Ethanol	298	3.5	0.654
DMSO	284	12.1	0.44
DMF	294	13.4	0.386
Ethyl acetate	280	19.15	0.22
Diethyl ether	287	8.4	0.117
Benzene	278	2.1	0.11
Toluene	-	-	0.099
Toluene	-	-	0.099

Table S2. Quantum yield measurements of CDs in different solvents.

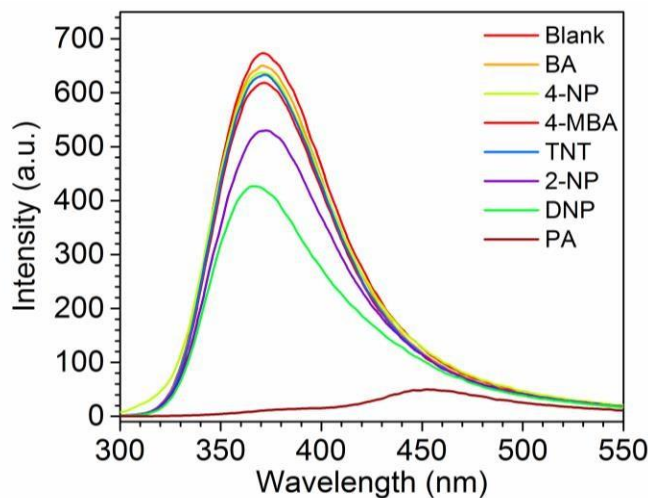


Fig.S10-Photoluminescence intensity variation of the quantum dots in the presence of different analytes. The excitation was done at 290 nm for all samples. The concentration of the analytes were fixed at 5 μM .

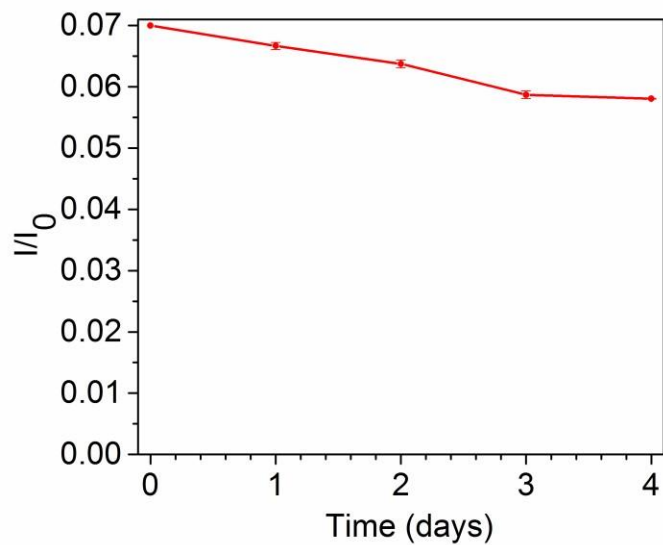


Fig.S11-The luminescence quenching of carbon dots as a function of time. The concentration of picric acid taken is $5\mu\text{M}$. The error bar represents the standard deviation of three measurements.

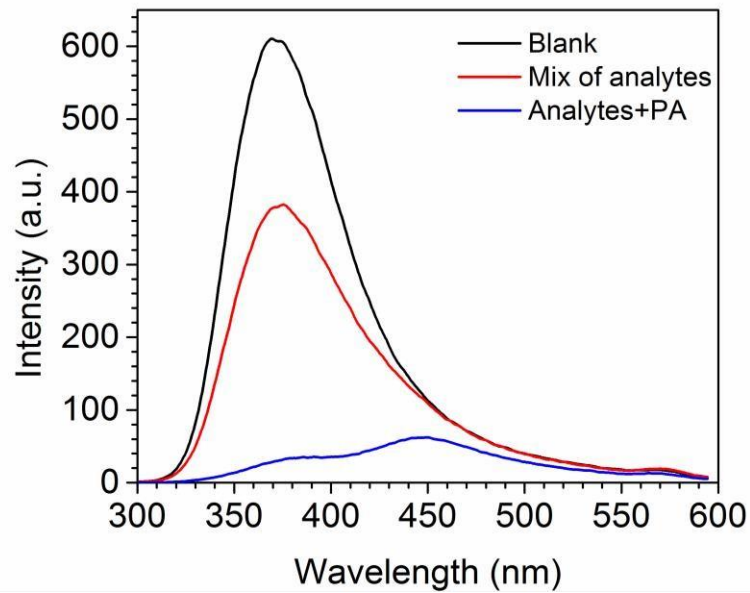


Fig. S12- Photoluminescence of carbon dots in the presence of picric acid and other interferents.

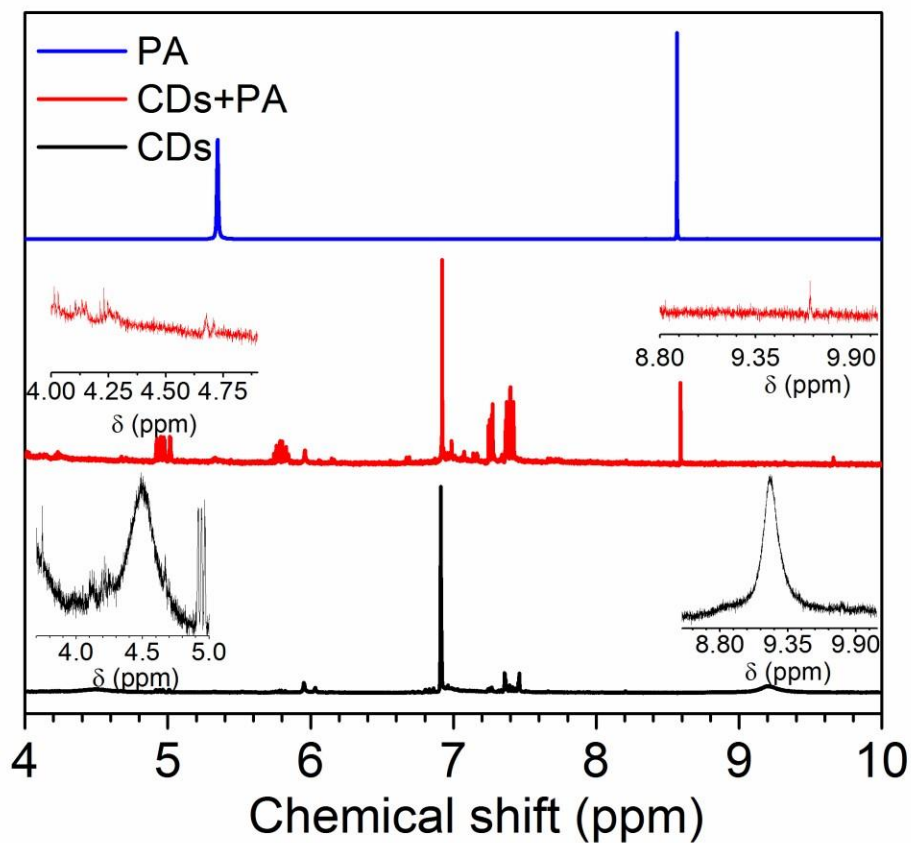


Fig.S13- ^1H NMR of carbon dots (black spectra). The spectra of picric acid alone, is represented by the blue curve, and the CDs - picric acid mixture (with picric acid concentration of about $5\mu\text{M}$), is represented by the red curve. The measurement was done after dispersing the solid sample in DMSO.

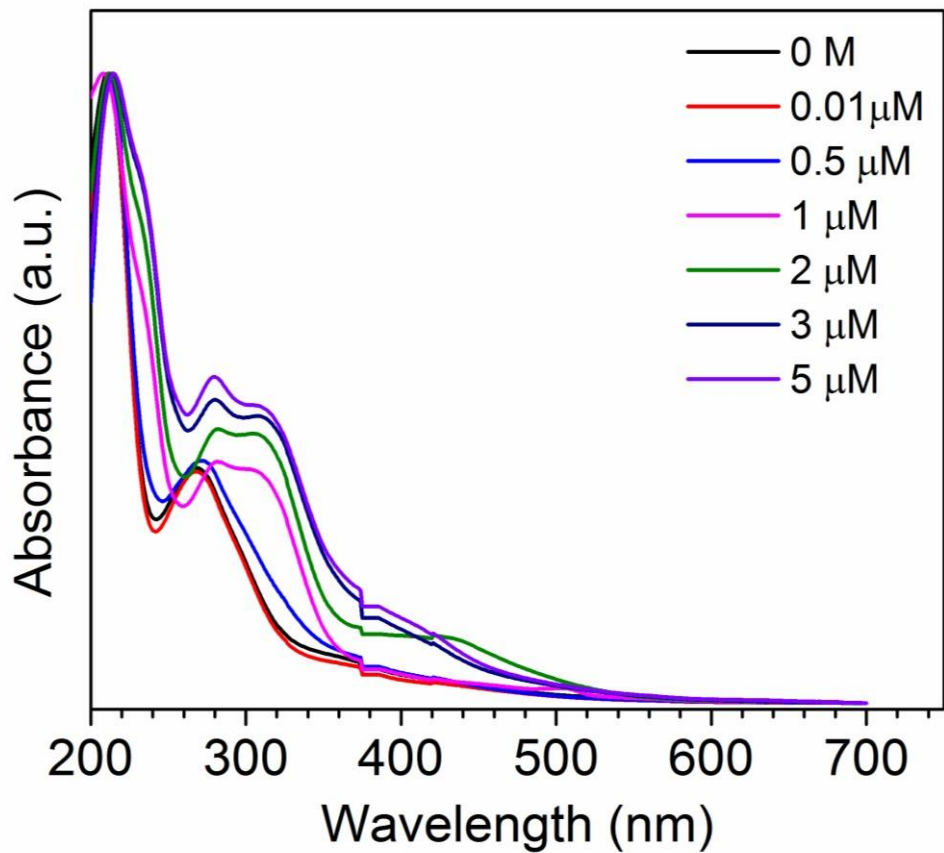


Fig.S14-UV-visible spectra of CDs without the analyte (0 M) and in the presence of the analyte (picric acid), in different concentrations.

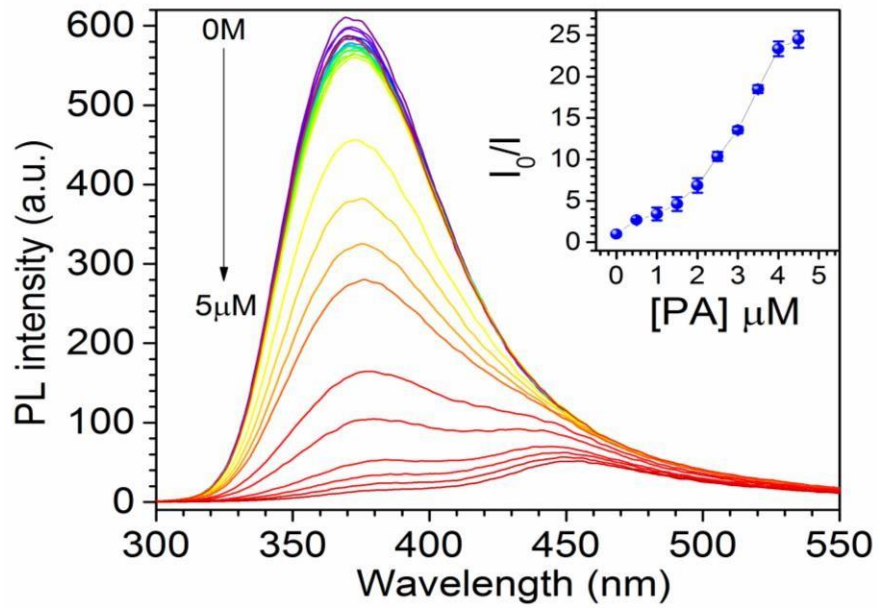


Fig.S15. PL spectra of the CDs in water at different concentrations of picric acid (zero to $5\mu\text{M}$). The inset shows the Stern-Volmer plot corresponding to the luminescence quenching. The excitation wavelength used was 290 nm. The error bar represents the standard deviation of five measurements.

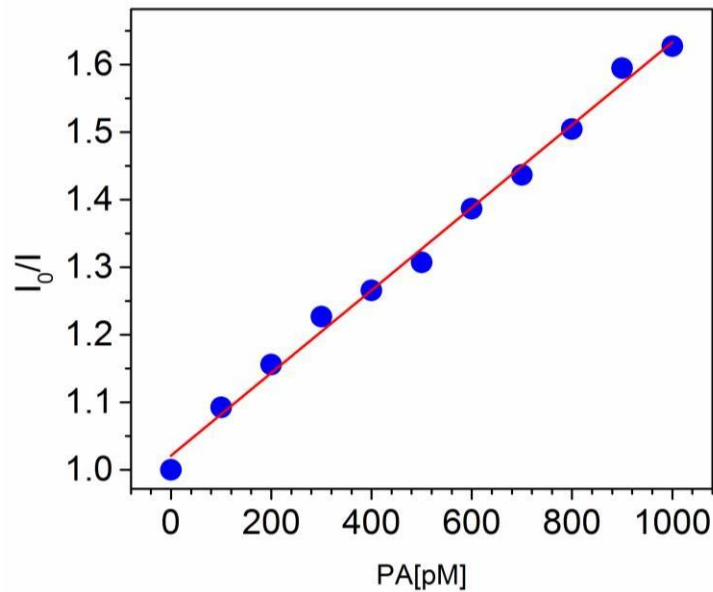


Fig.S16-Stern–Volmer plot representing linear range in the low concentration regime of quencher.

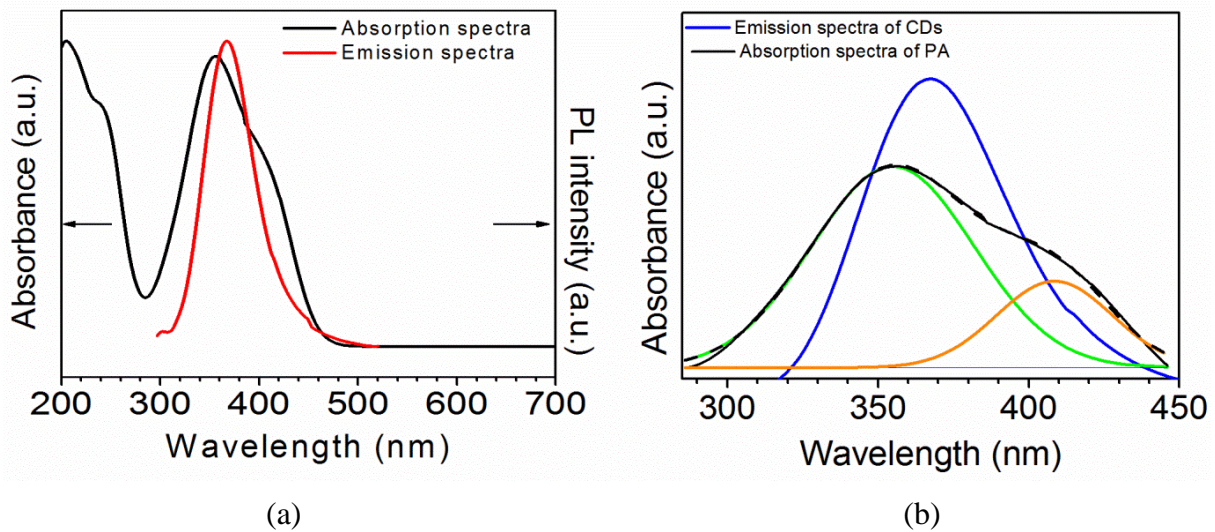


Fig.S17- (a) UV-Vis absorption spectra of aqueous solution of picric acid (black curve) and the PL spectra of CDs dispersed in water (red spectra). The PL spectra was obtained with excitation wavelength of 290 nm.(b)The absorption spectra of picric acid, deconvoluted at 355 nm (green) and 405 nm (orange).

Time-Correlated Single Photon Counting (TCSPC) Measurements

The photoluminescent decay curves were fitted using a two-exponential function using

$$\text{equation (1). } I(t) = A_1 e^{\frac{-t}{\tau_1}} + A_2 e^{\frac{-t}{\tau_2}} ; A_1 + A_2 = 1 \quad (1)$$

τ_1 , τ_2 are the decay time constants, and A_1, A_2 represent the normalised amplitudes of each component. The amplitude weighted average lifetime of the entire photoluminescence decay process was calculated using the equation (2)

$$\tau_{avg} = \frac{A_1 \tau_1^2 + A_2 \tau_2^2}{A_1 \tau_1 + A_2 \tau_2}, \quad (2)$$

where τ_{avg} is the average lifetime of the photoluminescence decay. The decay parameters of the CDs as estimated from the TCSPC data is included in Table S3.

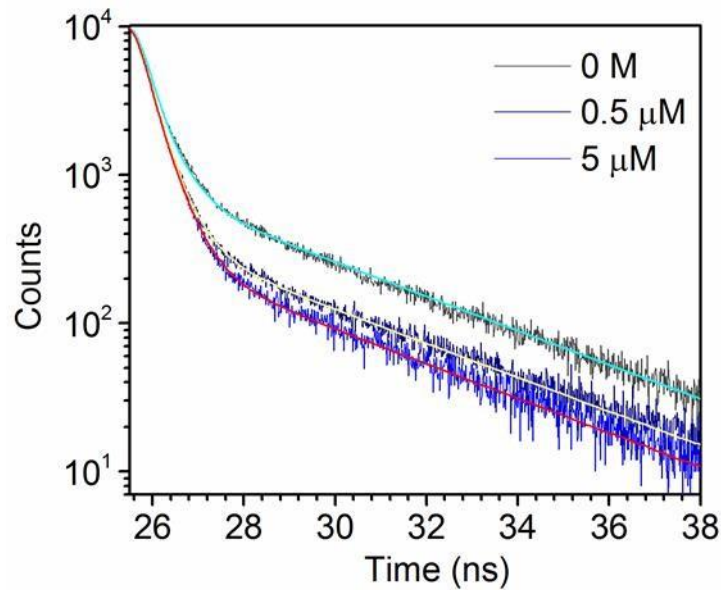


Fig.S18-The time-resolved PL decay curves for picric acid analysis, obtained using TCSPC technique. The PL decay of the CDs (0 μM) is represented by the grey curve. The remaining curves shows the decay curves of carbon dots in the presence of picric acid by varying the concentrations 0.5 μM and 5 μM .

	τ_1 (ns)	τ_2 (ns)	A_1	A_2	τ_{avg} (ns)
CDs	0.201	3.744	73.12	26.88	3.29
CDs + PA (0.5 μ M)	0.169	3.76	85.41	14.59	3.01
CDs + PA (5 μ M)	0.178	3.69	88.87	11.13	2.71

Table S3. The fitting parameters for the photoluminescence decay curves.

Quantum Yield (Q.Y.) calculation

The PL quantum yield was estimated using tryptophan as the standard, in water. The quantum yield of tryptophan was taken as, $Q_R \sim 0.14$;at 290 nm. The QY of the CDs were calculated according to the following equation, $Q = Q_R \frac{I}{I_R} \frac{A_R n^2}{A n_R^2}$; where Q and Q_R are the quantum yield of the sample and reference, I and I_R are the integrated PL intensities of the sample and the reference, A and A_R are the absorbance of the sample and the standard at the excitation wavelength; n and n_R are the refractive indices of the sample and reference respectively. The QY of the CDs are estimated to be about 7.6% at excitation wavelength of about $\lambda_{exc} \sim 290$ nm.